ACTA MECHANICA SINICA, Vol.8, No.4, November 1992 ISSN 0567-7718
Science Press, Beijing, China
Allerton Press, INC., New York, U. S. A.

EXPERIMENTAL INVESTIGATIONS OF HYPERVELOCITY IMPACT ONTO ALUMINIUM DUAL-PLATE STRUCTURE

Zhang Deliang (张德良) Tan Qingming (谈庆明) Zhao Chengxiu (赵成修)
Yang Yemin (杨业敏) Ge Xuezhen (葛学真) Zhang Qingming (张庆明)

(*Institute of Mechanics, Chinese Academy of Sciences, Beijing* 100080, *China*)

ABSTRACT : Dual-plate structure is very effective in the protection of space vehicle from hypervelocity impact. The experiments of Al projectile impacting Al dual targets at the velocity ranging over 2.5 — 7.0 km/s were systematically conducted. The damage effects were examined, including the perforation of the shield, the development of debris cloud and the general damage characteristics of the subplate. Many valuable experimental data and phenomena have been obtained

KEY WORDS: hypervelocity impact, dual-plate structure, perforation, damage, debris cloud, phase transition

I. INTRODUCTION

Along with the development of space technology, the life of space vehicles becomes longer. Therefore, it is more likely for them to be impacted by meteorites or space fragments with hypervelocity. About 40 years ago, F. L. Whipple[1] proposed to adopt a dual-plate structure in the design of space vehicle. Recent investigations indicated that with such structure a higher ratio of strength to weight could be achieved[2].

Utilizing a two-stage light-gas gun, the experiments of Al dual targets impacted by an Al spherical projectile were systematically investigated at the velocity ranging over 2.5 — 7.0 km/s. The damage characteristics of the dual targets, the developments of debris cloud formed by the impacting of projectile and shield and the phase transition were observed and analyzed. A large number of valuable experimental data and related complex phenomena were obtained and recorded.

II. EXPERIMENTAL FACILITIES AND MEASUREMENT METHODS

The experiments of hypervelocity impact were conducted by using a 20mm two-stage light-gas gun. The vacuum in the gun tube and the test section was about 10 — 30mm Hg. Both the projectile and the target were made of LY-12-CZ Al with density $\rho=2.7\text{g/cm}^3$, dynamic yield strength $Y=300\text{MPa}$. The diameter of the spherical projectile was $d_p=5.0\text{mm}$. The projectile velocities V_p ranged from 2.5 to 7.0km/s. The dual targets consisted of a shield (front target) and a subplate (back target, main structure) with a space between dual targets. The spacing gap L was 12cm and 20cm. The target thickness was within 1.0 — 8.0mm. The projectile velocity was exactly measured by using both optical method and contact-foil method. The perforation of the shield and the development of the debris cloud were recorded by two X-ray flash channels. The damage patterns remained on the shield —— hole and on the subplate —— craters were precisely measured with micrometer.

III. EXPERIMENTAL RESULTS AND MECHANICAL ANALYSES

1. Dual-plate Structure —— An Effective Type of Protective Structure for Hypervelocity Impact

In order to check the protective performance of dual targets, we observed and compared the penetration depth p of the dual target and the single thick target at different projectile velocities.

Received 9 January 1992

The results were shown in Fig. 1, in which p was the sum of the shield thickness and the maximum crater depth on the subplate. From Fig.1 it is clearly seen that as $V_p<3.5$km/s, the penetration depth of the dual target p_d is larger than that of the single target p_s. However, as $V_p>3.5$ km/s, p_d is smaller than p_s and becomes increasingly smaller with the increase of V_p. Thus, the protective performance of dual targets is obviously better. It can mainly be explained by the expanding debris cloud formed after impacting, which disintegrates the materials and disperses the flux acting on the subplate. Meanwhile, if V_p increases up to 7km/s, the melting effect will also play an important role.

2. Effect of Shield Thickness

The main factors affecting the protective performance are material properties and geometry parameters. In the present case of Al/Al impact, if we fix the projectile velocity at 5.3km/s and spacing at 12cm, but vary the shield thickness, we can find out experimentally the total target thickness for the critical penetration of the dual target. Fig. 2 shows the variation of dimensionless total target thickness $(t_s+t_b)/d_p$ with dimensionless shield thickness t_s/d_p. The point for $t_s=0$ corresponds to the degenerate case, in which the shield is absent. According to analysis the total thickness of the critical penetration for the single thick target is about 2.5 times of the crater depth. Because the experimental crater depth of the single target is 9.5mm[3], the value of $(t_s+t_b)/d_p$ is about 5.

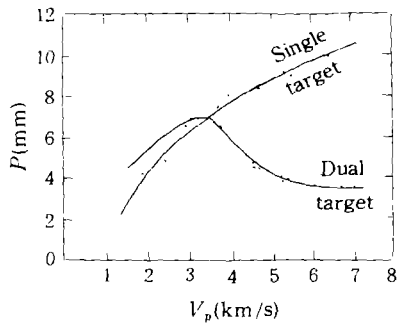

Fig. 1 Comparison of penetration depth of dual target and single thick target at various projectile velocities (t_s=3mm, t_b=5mm, L=12cm)

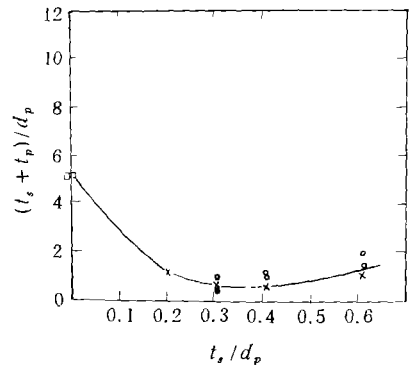

Fig. 2 Experimental results showing optimum shield thickness
(d_p=5mm, V_p=5.3km/s, L=12cm)
○ —— no penetration, × —— critical penetration, ◦ —— penetration
□ —— theoretical analysis

From Fig. 2 it can be found easily that $(t_s+t_b)/d_p$ has a minimum value, when $t_s/d_p=0.3$. It means that the protective performance of dual targets is optimum when $t_s/d_p=0.3$. Because the projectile diameter is 5mm, the optimum shield thickness should be near 1.5mm under our experimental conditions.

This experimental result can be interpreted as follows. The debris cloud is composed of the fragments of projectile and shield. In the range $t_s/d_p<0.3$, the main constituent is the projectile fragments. As t_s/d_p increases, the fragments of the projectile are seriously crashed more and more, so that the damage to the subplate is reduced. On the other hand, when $t_s/d_p>0.3$, the shield fragments constitute major part. When t_s/d_p increases, the crash of the shield becomes more difficult, so that the damage to the subplate is more serious due to the shield fragments of larger size. Hence, the optimum condition for the damage to the subplate, $t_s/d_p=0.3$, is just the result of the combination of these two effects.

3. Perforation of the Shield

When a projectile impacts a shield with hypervelocity, a hole is formed on the shield. Fig. 3 shows the perforating characteristics at different impact velocities. Fig. 4 indicates the relationship between hold diameter D and projectile velocity. Fig. 5 gives the relationship between hole

diameter and shield thickness. It is found that hole diameter increases with the increase of impact velocity and shield thickness. Meanwhile, Fig. 6 shows that our results agree well with those from Maiden & McMllian and McHugh[4].

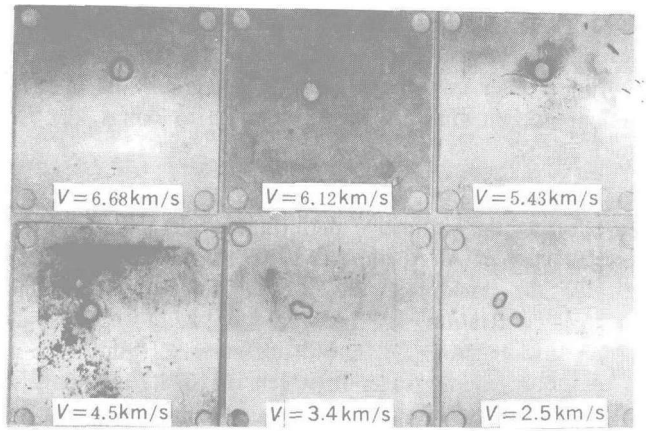

Fig. 3 Perforating characteristics at different impact velocities

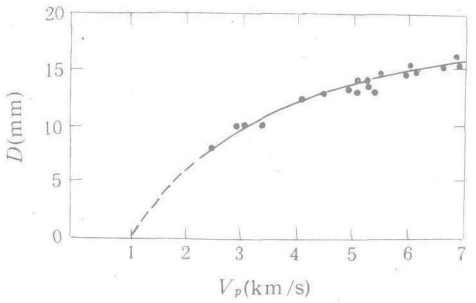

Fig. 4 Relationship between hole diameter and projectile velocity

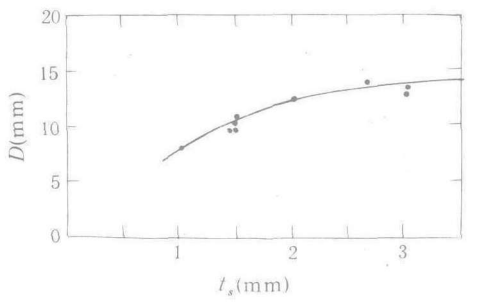

Fig. 5 Relationship between hole diameter and shield thickness

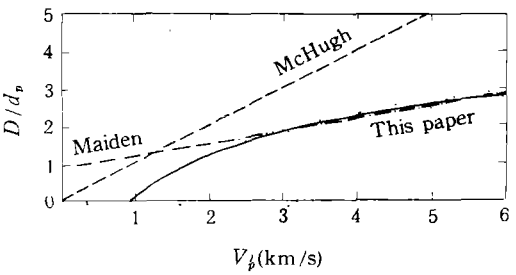

Fig. 6 Experimental results of the dependence of hole diameter on hypervelocity impact

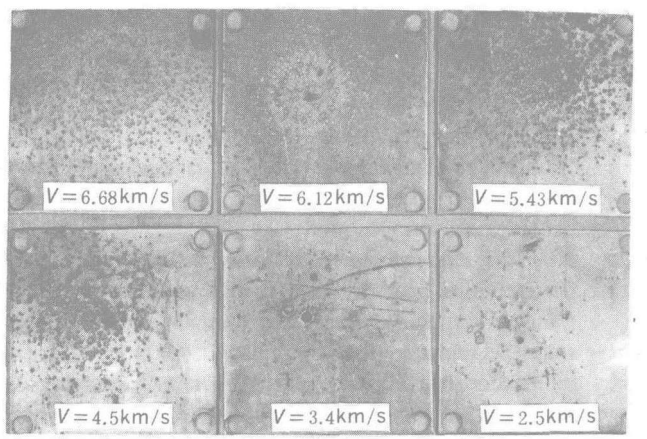

Fig. 7 Damage characteristics of the subplate at various projectile velocities

In addition, according to our previous experience, there must be a critical projectile velocity V_p, at which no perforation occurs. The resulting empirical formula for the hole diameter is

$$D/d_p = 0.96(\sqrt{\rho V_p^2/Y} - \sqrt{\rho V_p^{*2}/Y})^{0.5} \times (t_s/d_p)^{0.5}$$

in which V_p^* is taken as 1.0 km/s, Y is taken as 300 Mpa.

Table 1
Damage characteristics of subplate

Projectile velocity (km/s)	Dimension of max. subcrater (cm)		Pattern characteristics of ring position (cm)		Subcrater number N	Damage characteristics on the subplate
	diameter	depth	inner ring	outer ring		
2.5	6.0	1.5	/	/	$100>N>50$	no microcrater, relatively small number of subcraters of big size, irregular shape and with irregular distribution
3.4	6.0	2.5	/	/	$100>N>50$	no microcrater. number and depth of subcraters increase slightly, their shape and distribution begin to be regular.
4.5	5.0	1.8	/	/	$250>N>100$	no microcrater. number of subcraters increases obviously, in hemispherical shape, their distribution tends to take a ring pattern.
5.4	3.0	1.4	3.5	6.5	$500>N>250$	microcraters appear. number of subcraters increases continuously, but their depth becomes smaller, in hemispherical shape. two rings appear.
6.1	2.5	1.4	5.5	8.0	$1000>N>500$	microcrater number increases obviously subcrater number decreases, in hemispherical shape, with smaller size, large diameter ring, a ray pattern appears.
6.8	2.5	1.3	7.5	/	$N>1000$	micro craters are dense and overlapped, subcrater number deceases continuously, in hemispherical shape, larger diameter inner ring and outer ring disappears.

4. Damage Characteristics of the Subplate

When projectile velocity V_p is not very high, the main part of the cloud constituent is solid fragments. The size of the craters formed by impacting of solid fragments on the subplate is relatively big (about 1 — 6 mm in diameter). These craters are called "subcraters". As the projectile velocity is high enough, a number of smaller craters (less than 1 mm in diameter) are formed due to impacting of melt drops. These smaller craters are called "microcraters". At various projectile velocities the damage characteristics of the subplate are illustrated in Fig. 7. Fig. 8 shows the variations of the diameter and depth of the maximum subcrater with projectile velocity. The relevant parameters of the damage characteristics are listed in Table 1. Analyzing these damage characteristics, following comments can be made:

(1) The diameter of the maximum subcrater drops continuously down with the increase of projectile velocity. As V_p increases up to 6km/s, the trend of this decrease seems to slow down and finally to have stopped. The reason is that the sizes of the fragments become smaller with the increase of V_p. At the same time, the process of the phase transition occurs in the cloud.

(2) When $V_p < 3.5$km/s, the depth of the maximum subcraters slightly increases with the increase of V_p. However, when $V_p > 3.5$km/s, the depth decreases significantly as V_p increases.

When V_p=6.0km/s, this drop trend is basically stopped.

(3) The overall deformation of the subplate is related to the plate thickness. When V_p>5.0 km/s and the plate thickness is less than 5mm, the subplate will produce obvious bulge besides the local deformation.

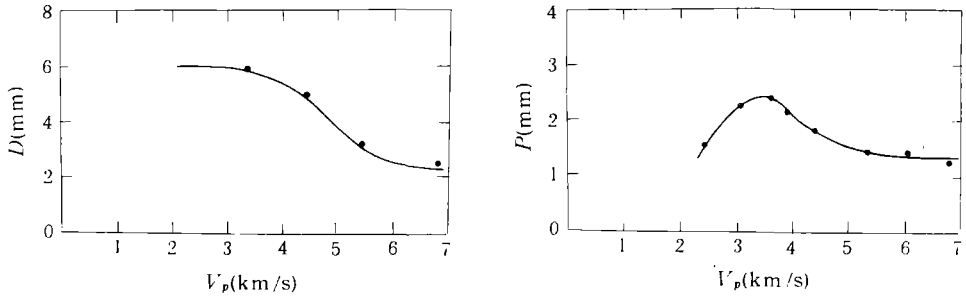

(a) The variation of the diameter of the maximum subcrater with projectile velocity(t_s= 3mm, t_b= 5mm, L = 12cm)

(b) The variation of the depth of the maximum subcrater with projectile velocity (t_s= 3mm, t_b= 5mm, L = 12 cm)

Fig. 8

(4) The distribution of the subcraters and the microcraters on the subplate has following characteristics: (i) There exist two obvious rings of the subcraters —— an inner ring and an outer ring. In these rings the subcraters are relatively deep. (ii) When V_p> 5km/s, besides a number of subcraters, there are much more microcraters in the inner ring. As V_p increases up to 7km/s, in the central area inside the inner ring, it can be seen that the microcraters are dense and overlapped. (iii) When V_p> 5km/s, the subcraters are in the hemisphere-like shape, the sizes are uniform, and the distribution of the subcraters is very regular. In addition, beyond the outer ring, a ray pattern of the subcraters appears.

From previous observations, it is concluded that when V_p> 3.5km/s, the damage on the subplate is reduced obviously and when the 5.0> V_p >7.0km/s, the distributions of the subcraters and the microcraters display the characteristic patterns.

5. Effect of Spacing Gap of Dual Targets

The experiments with the various projectile velocities and spacings were performed to examine spacing effects (V_p=3.4 and 5.4km/s and L=12 and 20cm). The damage characteristics are demostrated in Fig. 9.

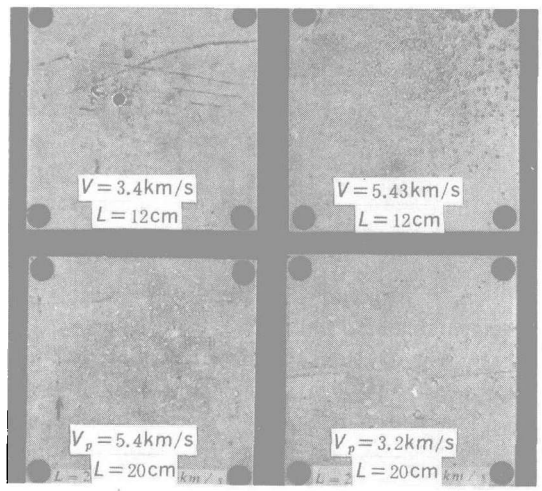

Fig. 9 Damage characteristics of different spacing gaps

Basically, the damage patterns on the subplates show that: (i) As L increases, the domain of two rings enlarges; but the number of the subcraters in unit area is adequately decreased. For example, as $V_p=5.4$km/s, $L=12$cm, the diameter of the inner ring is about 3.0cm. However, as $L=20$ cm at the same velocity, it is seen that the diameter of the inner ring is about 5.5cm and the outer ring disappears on the subplate. (ii) As L increases, the depth of the maximum subcrater basically does not change. (iii) As V_p increases, the inner ring expands gradually, such that the diameter of the inner ring goes from 5.0 to 5.6cm when V_p increases from 5.0 to 5.7km/s. Because the subcrater depth plays an important role in perforating subplate, the variation of the spacing is not important for the perforation damage to the subplate.

6. Formation and Development of Debris Clouds

The radiographs of debris cloud have been obtained using two X-ray flash channels[5, 6]. Fig. 10 (a) shows the view of Al/Al debris cloud with $V_p=5$km/s, $t_s=3$mm and flashing time triggered at 10μs and 25μs. Fig. 10 (b) shows the radiograph of Fe/Pb debris cloud with $V_p=6.3$ km/s, $t_s=3$mm and flashing time triggered at 28μs and 68μs. From the radiographs the following structural features are observed:

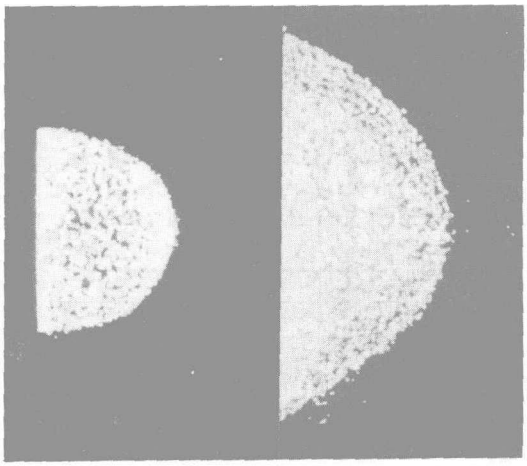

(a) Debris cloud radiograph of Al/Al impact(after treatment of microcomputer)

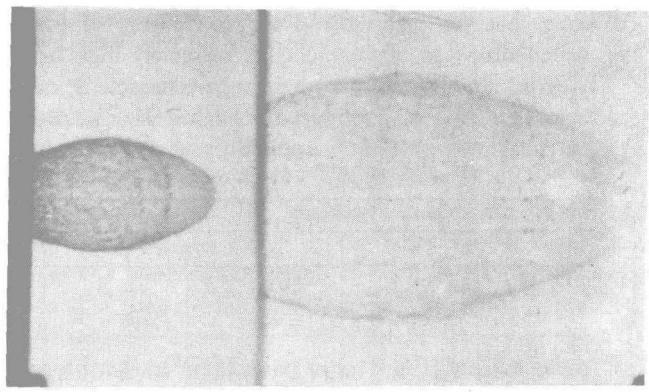

Debris cloud radiograph of Fe/Pb impact

Fig. 10

(1) From Fig. 10, it is evident that the mass is mainly concentrated in the head of the cloud.

(2) The appearance of the cloud seems to be a hollow bubble. The bubble expands and the outer shell thins down in the course of the forward motion.

(3) The indication of phase transition was observed clearly from the appearance of the debris cloud in radiograph 10(b) for Fe/Pb, however, it is obscure in radiograph 10(a) for Al/Al due to its low density.

The flying velocity of the head of debris cloud is an important parameter. From these radiographs we obtained the mean velocities of the head at various projectile velocities for the Al/Al case(see table 2). Obviously, the flying velocity of the head increases with the increase of projectile velocity. On the present condition, the flying velocity is about half as large as the projectile velocity.

Table 2

Relation between flying velocity of the head of debris cloud and projectile velocity

Experiment number	9111	9110	9103	9113
Projectile velocity(km/s)	5.7	5.0	4.2	3.2
Flying velocity of could head (km/s)	2.7	2.6	2.1	1.5

7. Characteristics of Phase Transition

According to the theory of shock wave the condition of the shock inducing phase transition of Al/Al impact was roughly estimated and listed in Table 3[7]. In view of this, on the present condition, i.e. $V_p<8.0$km/s, it is only possible to make Al melting, while the vaporization is impossible.

Analyzing the damage characteristics of the subplate is very helpful to obtain the information of phase transition. From Table 1 and Fig. 7 we have clearly known that when $V_p>5.0$ km/s, the damage patterns left on the subplate have distinct characteristics: the subcraters are obviously shallow, there are two rings of the subcraters, in which the subcraters are obviously large, in the central area microcraters are heavily overlapped. All of these damage characteristics are much more conspicuous, when $V_p=7.0$km/s. Preliminary analysis can indicate that these characteristics are related to the occurrence of melting.

In order to clarify further the viewpoint mentioned above, we need to observe the microstructure of the subcraters and the microcraters utilizing the electronic-scanning microscope. The typical overall and local morphology is shown in Fig. 11 for the subcraters and Fig. 12 for the microcraters with $V_p=5.8$km/s. From Fig. 11(a), it is clearly seen that there is locally melted material piled at the bottom of the subcraters. Fig. 11(b) (an enlargement of localized melted pile) shows that a ring pattern appears on the pile surface. Especially, from Fig. 12 on the surface of the microcraters covers a thin condensate layer. Therefore, it is reasonable to assume that the melting and the condensing of the thin layer result from the impact of either melted drops or of fragments of extremely high temperature. Through the above mentioned analyses of the macroscopic damage characteristics and the microscopic morphology, it can be concluded that melting occurs when $V_p>5.0$km/s.

Table 3

Shock condition for Al to be melted or vaporized[7]

Melting				Vaporization			
Incipient		Complete		Incipient		Complete	
Pressure (Mb)	Velocity (km/s)	Pressure (Mb)	velocity (km/s)	Prssure (Mb)	Velocity (km/s)	Pressure (Mb)	Velocity (km/s)
0.61 — 0.70	5.1 — 5.6	0.85 — 1.00	6.5 — 7.0	1.67	10.2	4.70	12.0

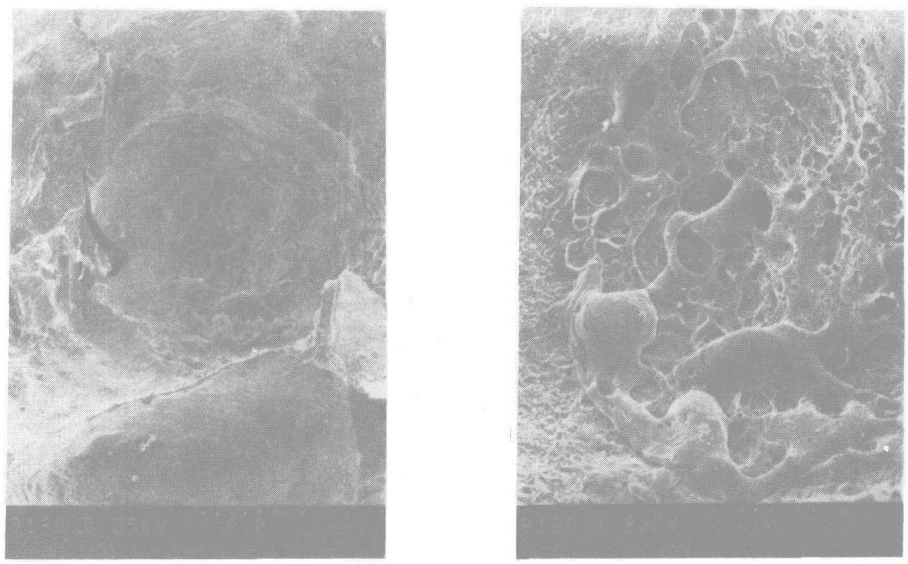

(a) Overall microscopic morphology (b) Local microscopic morphology

Fig. 11 Microscopie morphology of the subcraters

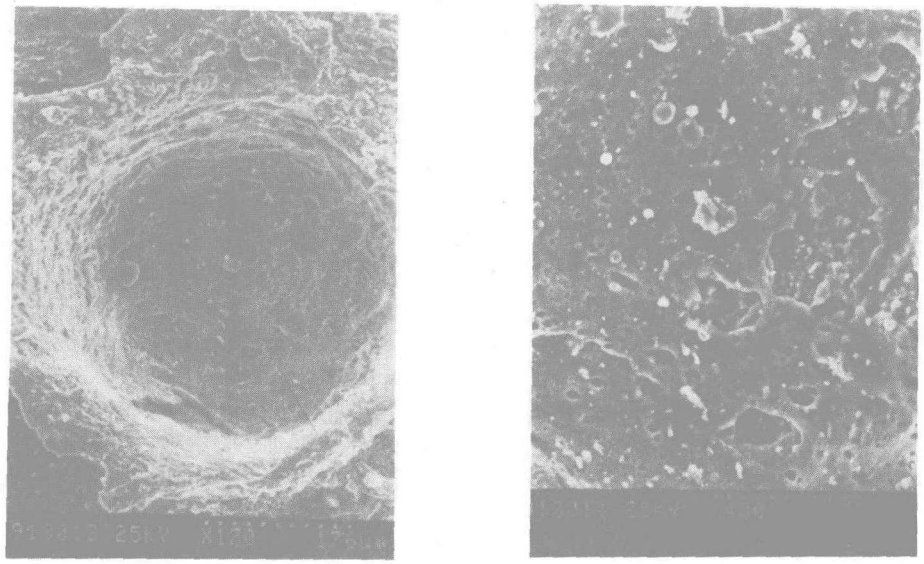

(a) Overall microscopic morphology (b) Local microscopic morphology

Fig. 12 Microscopic morphology of the microcraters

8. Relation Between Debris Cloud and Damage Characteristics of the Subplate.

Synthesizing the data of debris cloud development and damage pattern on remained subplate, an outline for the impact damage to dual targets was obtained. Fig. 13 presents the experimental results with two different spacings (L=12cm and 20cm), however, with the other parameters keeping same conditions (V_p=5.5km/s, t_s=3mm). The measured dimensions of the head of the debris cloud at two different exposure times and those of the inner rings on the subplate with two different spacings are shown in the same figure. Then, if we draw two straight lines tangential to the two inner rings (3.5cm and 5.6cm in diameter, respectively) and extend it forwards in uprange direction, it can be immediately found that the straight lines are just tangential to the original projectile and the two heads of the cloud (see Fig. 13). Although there is a certain error in measurements, however, from the result presented on Fig. 13, we deem that the subcraters and microcraters inside the inner ring are formed by impact of the fragments in the head of the could, which is produced by direct impact of the projectile on the shield and composed of the most part of projectile matter and a disk-like part of shield matter with approximately the same diameter as that of the projectile d_p.

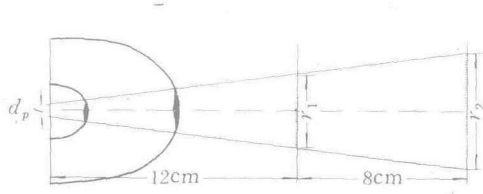

Fig. 13 Geometrical relation between inner ring on the subplate, debris cloud and projectile(V_p=5.5km/s, L=12 and 20cm, t_1=10μs, t_2=25μs)

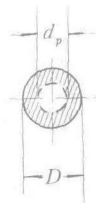

Fig. 14 A sketch of the relation between projectile diameter and hole diameter

Along with the increase of projectile velocity, when V_p>3.5km/s, the size of the fragments in the cloud reduces, while the number increases, so is the trend of the size of the subcraters on the subplate. As V_p>5.0km/s, melting occurs. At that time, the microcraters inside the inner ring are formed by the impact of the mixture of solid fragments and melted drops produced by

the direct impact of the projectile on the shield.

As is stated above, the punch hole diameter D is much larger than the projectile diameter d_p in the perforation of the shield, (see Fig. 14). For example, if $V_p=5.4$km/s. and $d_p=5$mm, then, $D=13.5$mm. A considerable amount of the shield material neighboring to the material punched forward by impact can be deformed and turned into a group of relatively big fragments due to the effect of the rarefaction and tension. These fragments are the main source to form the subcraters beyond the inner ring on the subplate and the main constituents of the outer thin shell of debris cloud.

IV. CONCLUSIONS

1. Compared with the single thick target, the dual-plate structure has higher ratio of strength to weight and better protective performance. Therefore, the latter is an effective type of protective structure for space vehicles.
2. The diameter of the perforated hole on the shield increases with the increase of projectile velocity and target thickness. In the range of $V_p=2.5$ — 7.0km/s, the empirical formula of hole diameter for Al/Al impact is

$$D/d_p=0.96\left(\sqrt{\rho V_p^2/Y}-\sqrt{\rho V_p^{*2}/Y}\right)^{0.5}\times\left(t_s/d_p\right)^{0.5}$$

where $V_p^*=1.0$km/s, $Y=300$MPa.
3. In the range of $V_p=5-7$km/s, the damage pattern on the subplate has distinct characteristics: two rings with deep "subcraters" and a central area with densely distributed microcraters. The range of $V_p=5$ — 7km/s corresponds to the transition of Al debris cloud from solid state to liquid state.
4. When the spacing of the dual targets is between 10 — 20cm, the spacing does not affect too much the maximum subcrater depth.
5. The mass of debris cloud is mainly concentrated in the head of debris cloud, while the rest of the mass is in an outer shell. The flying velocity of the cloud head is nearly the half as large as the projectile velocity.
6. The most dangerous domain of the damage on the subplate is the inner ring. The central area inside the inner ring is densely distributed by "microcraters" formed by the Al fine fragments or Al melted drops, which come from the punched a part of the shield and a most part of the projectile. The subcraters beyond the inner ring are contributed by the fragments which come from such part of shield material that is neighboring to the punched part by impact.

REFERENCES

1 Whipple F L. Meteorites and space travel, Astronautical Journal, 1947, 1161: 131
2 Fair H. Hypervelocity then and now. Int J Jmpact Eng, 1987, 5: 1 — 12
3 Cour-palais B G. Hypervelocity impact in metals, Glass and Composites. Int J Impact Eng, 1987, 5: 221 — 237
4 Gehring, J W. Theory of impact on thin target and shield and correlation with experiment. In: High-velocity Impact Phenomena, Chapter IV, pp 105 — 156, edited by R. Kinslow, New York London: Academic Press. Inc., 1970.
5 Piekutowski A J. Debris cloud generated by hypervelocity impact of cylindrical projectiles with thin aluminium plates, Int J Impact Eng, 1987, 5: 509 — 519
6 Piekutowski A J. A simple dynamic model for the formation of debris clouds, Int J Impact Eng, 1990, 10: 453 — 471
7 Swift, H. F. Hypervelocity Impact Mechanics, in Impact Dynamics, edited by J. A. Zucas et al., John Wiley & Sons, N. Y. C., 1982.